J. Phys. B: At. Mol. Opt. Phys. 23 (1990) 1491-1499. Printed in the UK

Ionisation and electron capture in collisions of H^+ and He^{2+} ions with carbon monoxide

M B Shah and H B Gilbody

Department of Pure and Applied Physics, The Queen's University of Belfast, Belfast, UK

Received 4 December 1989

Abstract. A crossed-beam technique employing time-of-flight analysis and coincidence counting of the collision products has been used to identify and obtain cross sections for the main channels in collisions of 10-98 keV amu^{-1} H^+ and 6.7-65 keV amu^{-1} He^{2+} ions with carbon monoxide. Separate cross sections for non-dissociative and dissociative electron capture, transfer ionisation and ionisation involving the production of CO^+, C^+, O^+, CO^{2+}, C^{2+} and O^{2+} ions have been determined for the first time. While non-dissociative electron capture and ionisation are dominant in the energy ranges considered, transfer ionisation is also important, particularly in the case of He^{2+} impact.

1. Introduction

In previous work in this laboratory (Shah and Gilbody 1981) we developed a crossed-beam technique for high-precision studies of the ionisation of atomic hydrogen by ion impact. In subsequent measurements with molecular hydrogen, the same experimental (Shah and Gilbody 1982, Shah *et al* 1989) approach has been used to obtain cross sections for non-dissociative and dissociative channels for both electron capture and ionisation over a wide energy range.

In the present work we have used the same experimental approach to study both electron capture and ionisation in collisions of H^+ and $^3He^{2+}$ with CO at energies within the ranges 10-98 keV amu^{-1} and 6.7-65 keV amu^{-1} respectively. Apart from the fundamental interest, the results are relevant to a better understanding of the interaction of the solar wind with cometary atmospheres. For example, in the data from recent studies of comet Halley using instrumented spacecraft, there is a need for reliable cross sections to explain the apparently high rate of charge exchange observed in interactions of the He^{2+} component of the solar wind with cometary gas (Neugenbauer 1988).

Cross sections have been separately determined for the following processes (where X^{z+} is either H^+ or He^{2+}) involving electron capture:

non-dissociative electron capture

$$X^{z+} + CO \rightarrow X^{(z-1)+} + CO^+ \tag{1a}$$

dissociative electron capture

$$X^{z+} + CO \rightarrow X^{(z-1)+} + C^+ + O \tag{1b}$$

$$\rightarrow X^{(z-1)+} + C + O^+ \tag{1c}$$

0953-4075/90/091491+09$03.50

non-dissociative transfer ionisation

$$X^{z+} + CO \rightarrow X^{(z-1)+} + CO^{2+} + e \tag{1d}$$

dissociative transfer ionisation

$$X^{z+} + CO \rightarrow X^{(z-1)+} + C^{+} + O^{+} + e \tag{1e}$$

$$\left.\begin{aligned} &\rightarrow X^{(z-1)+} + C^{2+} + O + e \\ &\rightarrow X^{(z-1)+} + C^{2+} + O^{+} + 2e \\ &\rightarrow X^{(z-1)+} + C^{2+} + O^{2+} + 3e \end{aligned}\right\}. \tag{1f}$$

Cross sections for the following processes involving ionisation have also been obtained

$$X^{z+} + CO \rightarrow X^{z+} + CO^{+} + e \tag{2a}$$

$$\rightarrow X^{z+} + C^{+} + O + e \tag{2b}$$

$$\rightarrow X^{z+} + C + O^{+} + e. \tag{2c}$$

Previous studies of electron capture in H^+-CO and He^{2+}-CO collisions have been very limited. The condenser plate method has been used by Poulizac *et al* (1967) for 5-50 keV amu^{-1} H^+ ions and by Rudd *et al* (1983, 1985) for 5-4000 keV amu^{-1} H^+ and 5-300 keV amu^{-1} $^3He^{2+}$ ions to obtain data on slow ion and electron production that can be related to total electron capture and ionisation cross sections. In previous work in this laboratory (Browning and Gilbody 1968) a mass spectrometric analysis of the slow ion products of 5-45 keV amu^{-1} H^+-CO collisions provided cross sections for formation of CO^+, C^+, O^+, CO^{2+}, C^{2+} and O^{2+}. However, unlike the present work, it was not possible to separately determine cross sections for particular electron capture or ionisation channels.

2. Experimental approach

The experimental arrangement was similar to that used in our previous studies of H_2 (Shah and Gilbody 1982, Shah *et al* 1989) and only a summary of the essential features needs to be given here.

A momentum-analysed beam of either H^+ or $^3He^{2+}$ ions of the required energy was arranged to intersect (at right angles) a thermal energy beam of carbon monoxide in a differentially pumped high vacuum ($\sim 2 \times 10^{-7}$ Torr) region. The CO beam was formed by utilising a bunch of hypodermic needles each 10 mm long and 1 mm in diameter set into a thin-walled 4 mm diameter tube.

The slow ions and electrons formed as collision products in the beam intersection region were collected by a transverse electric field applied between two grids and separately counted by particle multipliers. As in our previous work, particular care was taken to ensure that the small deflection of the primary beam by the extraction field caused a negligible change in the effective collision volume. Product CO^+, CO^{2+}, C^+, O^+, C^{2+} or O^{2+} ions were recorded with a high and uniform efficiency and could be selectively identified and distinguished from background gas products by their different times of flight to the particle counter in accord with their charge-to-mass ratios.

The slow ion products from the ionisation processes (2) could be separately distinguished from those from the electron capture processes (1) by counting them in coincidence with the electrons from the same events. In addition, by deploying a third particle multiplier beyond the beam intersection region as in our previous work, fast $X^{(z-1)+}$ product ions (selected by electrostatic deflection) could be counted in coincidence with slow mass-analysed product ions. In this way, the separate contributions from the electron capture processes (1) could be obtained. The time-of-flight spectra based on slow-ion-electron coincidences or slow-ion-fast-ion coincidences both included contributions from the transfer ionisation processes (1*d*-*f*). In order to separately assess cross sections for the latter, we recorded triple coincidences between the selected slow product ions, fast $X^{(z-1)+}$ ions and electrons arising from the same events.

Open-ended multipliers were used to count the electrons and fast $X^{(z-1)+}$ product ions. However, unlike our previous work, we used a particle detector of the type described by Daly (1960) to count the slow product ions. This utilises a scintillation counter to record secondary electrons ejected by the ions from a metal electrode maintained at a high negative potential. An operating potential of 26 keV ensured a counting efficiency close to unity for all the slow ion species considered. This was an important consideration in separating the contributions of the same product ion to different processes.

A typical time-of-flight spectrum for slow-ion-fast-ion coincidences in He^{2+}-CO collisions shown in figure 1 illustrates the satisfactory degree of resolution obtainable for electron capture channels involving CO^+, CO^{2+}, C^+, O^+, C^{2+} and O^{2+} production. Dissociative processes which involve a spread in both the energy and initial directions of the fragment ions necessarily produce broader peaks than those arising from

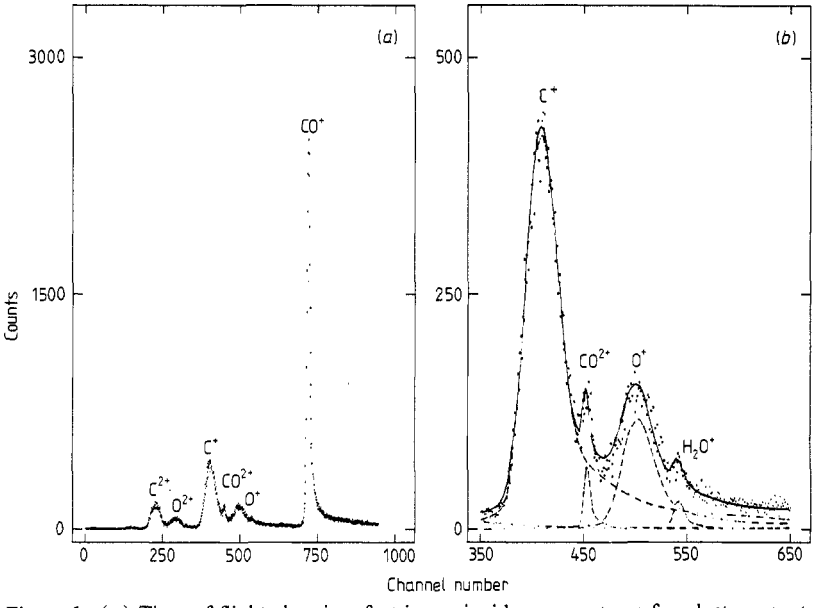

Figure 1. (*a*) Time-of-flight slow-ion-fast-ion coincidence spectrum for electron capture in 33 keV amu^{-1} He^{2+}-CO collisions. (*b*) Expanded section of the spectrum illustrating our curve fitting procedure for the C^+, O^+, CO^{2+} and H_2O^+ peaks.

Table 1. Cross sections (in units of 10^{-16} cm^2) for electron capture processes (1*a*–*c*), for transfer ionisation processes (1*d*–*e*) and for ionisation processes (2*a*–*c*) in H^+–CO collisions.

Energy (keV amu^{-1})	Electron capture processes			Transfer ionisation processes			Ionisation processes		
	(1*a*)	(1*b*)	(1*c*)	(1*d*)	(1*e*)	(1*f*)	(2*a*)	(2*b*)	(2*c*)
10	9.96 ± 0.65	—	—	—	—	—	1.32 ± 0.05	—	—
13	8.40 ± 0.57	1.10 ± 0.17	0.53 ± 0.07	0.096 ± 0.012	0.70 ± 0.08	0.070 ± 0.012	1.56 ± 0.05	1.19 ± 0.12	0.34 ± 0.05
16	7.56 ± 0.36	0.96 ± 0.13	0.46 ± 0.06	0.119 ± 0.013	0.86 ± 0.07	0.094 ± 0.011	1.81 ± 0.06	1.06 ± 0.10	0.35 ± 0.05
20	6.24 ± 0.17	0.90 ± 0.10	0.38 ± 0.05	0.109 ± 0.009	0.83 ± 0.05	0.091 ± 0.010	2.23 ± 0.06	1.19 ± 0.10	0.38 ± 0.05
26	5.00 ± 0.10	0.80 ± 0.09	0.43 ± 0.06	0.085 ± 0.007	0.68 ± 0.04	0.101 ± 0.010	2.67 ± 0.06	1.27 ± 0.09	0.37 ± 0.05
32	4.07 ± 0.08	0.65 ± 0.07	0.38 ± 0.04	0.078 ± 0.005	0.68 ± 0.03	0.112 ± 0.09	3.36 ± 0.06	1.38 ± 0.07	0.38 ± 0.05
40	3.00 ± 0.06	0.55 ± 0.06	0.36 ± 0.05	0.062 ± 0.005	0.55 ± 0.03	0.104 ± 0.09	3.72 ± 0.07	1.43 ± 0.07	0.40 ± 0.04
50	2.34 ± 0.06	0.49 ± 0.06	0.31 ± 0.04	0.043 ± 0.004	0.49 ± 0.03	0.097 ± 0.08	3.77 ± 0.07	1.22 ± 0.07	0.36 ± 0.04
62	1.68 ± 0.04	0.40 ± 0.04	0.25 ± 0.03	0.035 ± 0.004	0.37 ± 0.02	0.079 ± 0.07	3.91 ± 0.07	1.20 ± 0.07	0.36 ± 0.04
78	1.09 ± 0.04	0.28 ± 0.03	0.18 ± 0.02	0.0216 ± 0.0024	0.28 ± 0.02	0.064 ± 0.06	3.94 ± 0.07	1.09 ± 0.06	0.32 ± 0.04
98	0.68 ± 0.03	0.19 ± 0.03	0.11 ± 0.02	0.0132 ± 0.0012	0.16 ± 0.01	0.035 ± 0.03	3.91 ± 0.07	1.04 ± 0.05	0.31 ± 0.04

Table 2. Cross sections (in units of 10^{-16} cm^2) for electron capture processes (1*a*–*c*), for transfer ionisation processes (1*d*–*e*) and for ionisation processes (2*a*–*c*) in He^{2+}–CO collisions.

Energy (keV amu^{-1})	Electron capture processes			Transfer ionisation processes			Ionisation processes		
	(1*a*)	(1*b*)	(1*c*)	(1*d*)	(1*e*)	(1*f*)	(2*a*)	(2*b*)	(2*c*)
6.67	8.71 ± 0.15	—	—	—	—	—	—	—	—
8.67	10.8 ± 0.2	—	—	—	—	—	—	—	—
10.7	11.8 ± 0.2	1.43 ± 0.16	0.50 ± 0.08	0.10 ± 0.02	1.99 ± 0.08	1.13 ± 0.06	0.47 ± 0.04	—	—
13.3	12.2 ± 0.2	1.38 ± 0.17	0.52 ± 0.07	0.13 ± 0.02	2.27 ± 0.09	1.44 ± 0.07	0.56 ± 0.04	0.40 ± 0.12	—
17.3	11.8 ± 0.2	1.68 ± 0.18	0.60 ± 0.07	0.16 ± 0.02	2.27 ± 0.08	1.58 ± 0.08	0.94 ± 0.05	0.55 ± 0.13	0.12 ± 0.05
21.3	11.2 ± 0.2	1.87 ± 0.18	0.62 ± 0.07	0.19 ± 0.02	2.32 ± 0.08	1.75 ± 0.07	1.43 ± 0.06	0.40 ± 0.12	0.08 ± 0.05
26.7	9.67 ± 0.17	1.94 ± .017	0.66 ± 0.07	0.20 ± 0.02	2.27 ± 0.08	1.81 ± 0.07	2.53 ± 0.08	0.72 ± 0.14	0.12 ± 0.05
33.3	7.88 ± 0.13	1.82 ± 0.18	0.62 ± 0.08	0.21 ± 0.02	2.47 ± 0.08	2.10 ± 0.07	3.59 ± 0.09	0.60 ± 0.13	0.13 ± 0.05
42.7	5.83 ± 0.12	1.75 ± 0.17	0.60 ± 0.07	0.18 ± 0.02	2.29 ± 0.08	2.00 ± 0.07	5.24 ± 0.12	0.88 ± 0.12	0.22 ± 0.06
52.0	4.31 ± 0.11	1.67 ± 0.15	0.56 ± 0.07	0.14 ± 0.02	2.09 ± 0.06	2.04 ± 0.06	6.02 ± 0.13	1.08 ± 0.12	0.36 ± 0.06
65.3	3.05 ± 0.09	1.57 ± 0.15	0.46 ± 0.07	0.12 ± 0.02	1.75 ± 0.07	1.80 ± 0.07	6.64 ± 0.13	1.54 ± 0.14	0.38 ± 0.06

non-dissociative processes. In order to deconvolute the contributions from the tails of overlapping peaks, each peak was fitted by three Gaussian functions of the form

$$\sum_{k=1}^{3} A_k x^2 \exp\left[-\left(\frac{x-x_0}{a_k}\right)^2\right]$$

for channel numbers x with peak at x_0 and with empirically selected values of fitting parameters $A_2 = 0.16A_1$, $A_3 = 0.05A_1$, $a_2 = 2.54a_1$ and $a_3 = 8.2a_1$. The results in figure 1(*b*) show the results of this fitting procedure for the closely spaced peaks C^+, CO^{2+}, O^+ and the impurity H_2O^+ peak. Respective values of the fitting parameters A_1, x_0 and a_1 were 200, 393 and 25 for C^+, 32, 450 and 5 for CO^{2+}, 55, 487 and 24.5 for O^+ and 14, 537 and 8 for H_2O^+.

Relative cross sections for both H^+ and He^{2+} impact obtained from an analysis of the time-of-flight spectra were normalised by reference to the absolute total slow ion production cross sections σ_+ previously measured by Rudd *et al* (1983) for H^+-CO collisions using the condenser plate method. On the basis of the uncertainties quoted for their measurements of cross sections σ_- for electron production, we estimate an average uncertainty of 13% in their measurements of σ_+ in the H^+ impact energy range 25–100 keV. This provides an estimated uncertainty of ±15% in the absolute values of our normalised cross sections for both the capture channels (1.1)–(1.6) and ionisation channels (2.1)–(2.3). Tables 1 and 2 list our measured cross sections for specific channels for H^+ and He^{2+} impact. The estimated uncertainties in the tabulated cross sections reflect the degree of reproducibility of the time-of-flight spectra and, for peaks other than CO^+, uncertainties arising from the deconvolution procedure. As noted earlier, the time-of-flight spectra based on slow-ion–electron coincidences and on slow-ion–fast-ion coincidences both included contributions from transfer ionisation. As a result, our cross section tabulations include additional uncertainties in the electron capture cross sections for (1*b*) and (1*c*) and in the ionisation cross sections for (2*b*) and (2*c*) as a result of subtracting cross sections for the transfer ionisation process (1*e*).

3. Results and discussion

As noted in section 1, previous experimental measurements have not provided detailed information on specific processes. All the previous data for proton impact are compared with the results of the present measurements in figure 2. The agreement between cross sections σ_+ for slow ion production and σ_- for electron production measured by Rudd *et al* (1983) and by Poulizac *et al* (1967) can be seen to be not entirely satisfactory, especially within the present energy range. Our values of σ_+, which are synthesised from the sum of the relevant individual cross sections, are (as already noted) normalised to the values due to Rudd *et al* (1983). Agreement between values of σ_- measured by the latter workers and our synthesised values of σ_- can be seen to be very good.

We also show in figure 2 the cross sections previously measured in this laboratory by Browning and Gilbody (1968) for CO^+, C^+ and O^+ production. These cross sections were normalised to the values of σ_+ measured by Poulizac *et al* (1967) which are somewhat smaller than the more recent and accurate values due to Rudd *et al* (1983) in the present energy range. This partly accounts for the generally poor agreement with cross sections for CO^+, C^+ and O^+ production synthesised from the present measurements. In addition, unlike the present crossed-beam technique, it was much

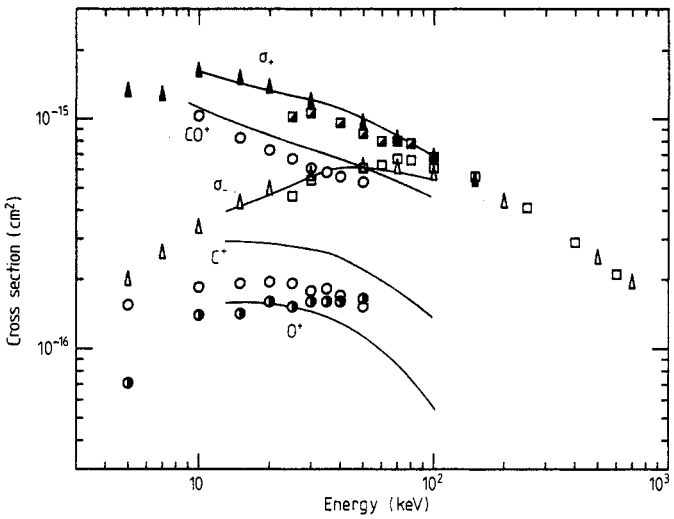

Figure 2. Cross sections for slow-ion and electron production in H^+-CO collisions. ▲, σ_+ (Rudd *et al* 1983); △, σ_- (Rudd *et al* 1983); ◪, σ_+ (Poulizac *et al* 1967); □, σ_- (Poulizac *et al* 1967). ○, ○, ◑; CO^+, C^+, O^+ production cross sections (Browning and Gilbody 1968). ——, cross sections σ_+, σ_- and for CO^+, C^+ and O^+ production synthesised from present data.

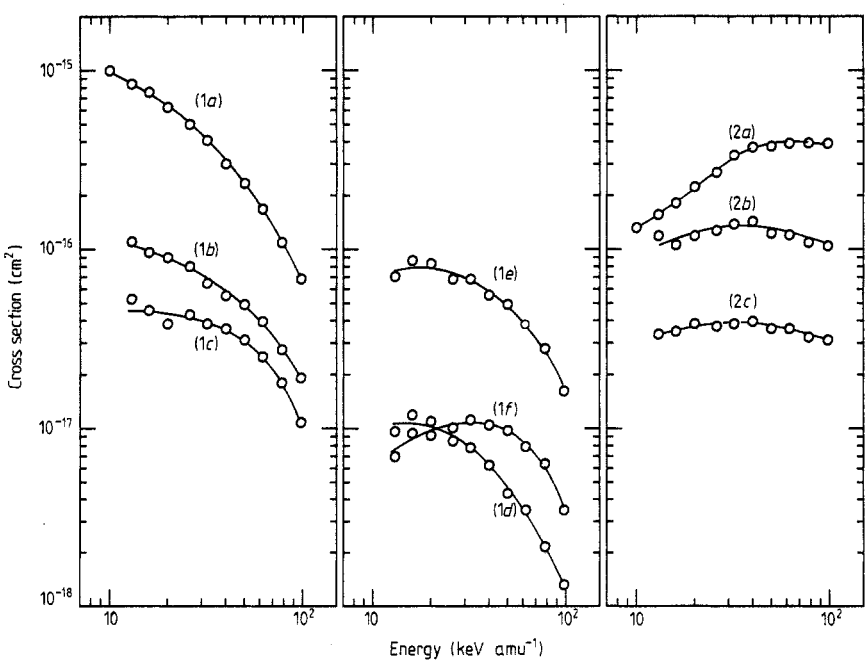

Figure 3. Cross sections for electron capture processes (1*a*-*c*) for transfer ionisation processes (1*d*-*f*) and for ionisation processes (2*a*-*c*) in H^+-CO collisions.

more difficult in the experiments of Browning and Gilbody (1968) to ensure that the slow ion collision products could be collected with a high and uniform efficiency.

Our cross sections for the specific processes (1*a-c*) for electron capture, (1*d-f*) for transfer ionisation and (2*a-c*) for ionisation are shown in figures 3 and 4 for H^+ and He^{2+} impact respectively. The various electron capture and ionisation processes all make significant contributions within the present energy range.

For proton impact, cross sections for the electron capture processes (1*a-c*) are increasing with decreasing impact energy down to our low-energy limits. Cross sections for the non-dissociative electron capture process (1*a*) are large and 7.6 and 15.8 times greater than the dissociative electron capture processes (1*b*) and (1*c*) respectively at 13 keV amu^{-1}. In the case of ionisation, cross sections for processes (2*a-c*) attain peak values within the present range with the non-dissociative ionisation process (2*a*) dominant. At 98 keV amu^{-1}, cross sections for (2*a*) are 3.8 and 12.6 times greater than those for (2*b*) and (2*c*) respectively. In the case of transfer ionisation, process (1*e*) for $C^+ + O^+$ production is clearly dominant. The peak value of the cross section (1*d*) for CO^{2+} production is only 0.14 times the cross section for (1*e*) at the same energy. Similarly the peak value of the cross section for (1*f*) which leads to C^{2+} production is only 0.17 times the cross section for (1*e*) at the same energy.

The cross sections for He^{2+} impact (figure 4) exhibit a behaviour which is generally similar to the corresponding cross sections for H^+ impact although peak values are shifted towards higher impact velocities. Transfer ionisation is also relatively more important. In particular it is interesting to note that cross sections for the transfer ionisation process (1*f*) for C^{2+} production become equal to those for (1*e*) for $C^+ + O^+$ production at our high-energy limit. Cross sections (1*d*) for CO^{2+} production are relatively small.

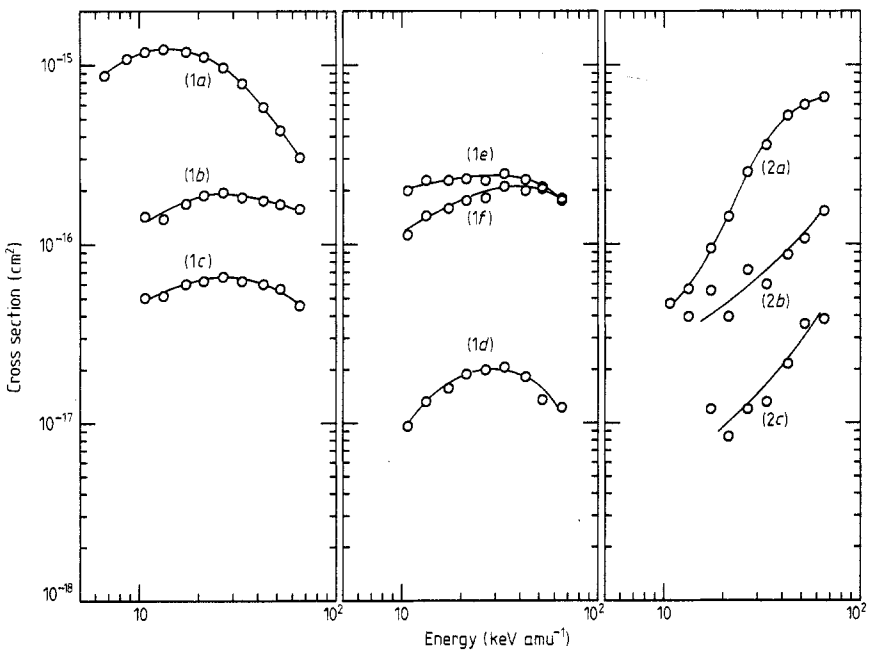

Figure 4. Cross sections for electron capture processes (1*a-c*) for transfer ionisation processes (1*d-f*) and for ionisation processes (2*a-c*) in He^{2+}-CO collisions.

Our measurements illustrate the rich variety of electron capture and ionisation channels in both H^+-CO and He^{2+}-CO collisions and provide a quantitative assessment of the individual processes leading to particular target production ions. No theoretical studies of these processes are available at this time.

Acknowledgments

This research was supported by a Research Grant from the Science and Engineering Research Council.

References

Browning R and Gilbody H B 1968 *J. Phys. B: At. Mol. Phys.* **1** 1149
Daly N R 1960 *Rev. Sci. Instrum.* **22** 166
Neugenbauer M M 1988 *Bull. Am. Phys. Soc.* **33** 971
Poulizac M C, Desesquelles J and Dufay M 1967 *Ann. Astrophys.* **30** 301
Rudd M E, DuBois R D, Toburen L H, Ratcliffe C A and Goffe T V 1983 *Phys. Rev.* A **28** 3244
Rudd M E, Goffe T V and Itoh A 1985 *Phys. Rev.* A **32** 2128
Shah M B and Gilbody H B 1981 *J. Phys. B: At. Mol. Phys.* **14** 2361
—— 1982 *J. Phys. B: At. Mol. Phys.* **15** 3441
Shah M B, Gilbody H B and McCallion P 1989 *J. Phys. B: At. Mol. Opt. Phys.* **22** 3037